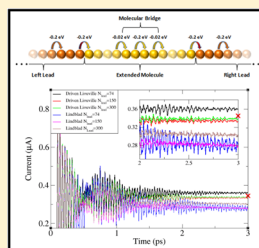


Driven Liouville von Neumann Equation in Lindblad Form

Oded Hod,^{*,†} César A. Rodríguez-Rosario,[‡] Tamar Zelovich,[†] and Thomas Frauenheim[‡][†]Department of Physical Chemistry, School of Chemistry, The Raymond and Beverly Sackler Faculty of Exact Sciences and The Sackler Center for Computational Molecular and Materials Science, Tel Aviv University, Tel Aviv 6997801, Israel[‡]Bremen Center for Computational Materials Science, University of Bremen, Am Falturm 1, Bremen, 28359, Germany

ABSTRACT: The Driven Liouville von Neumann approach [*J. Chem. Theory Comput.* **2014**, *10*, 2927–2941] is a computationally efficient simulation method for modeling electron dynamics in molecular electronics junctions. Previous numerical simulations have shown that the method can reproduce the exact single-particle dynamics while avoiding density matrix positivity violation found in previous implementations. In this study we prove that in the limit of infinite lead models the underlying equation of motion can be cast in Lindblad form. This provides a formal justification for the numerically observed density matrix positivity conservation.



$$\dot{\rho}(t) = -\frac{i}{\hbar}[H, \rho] + \mathcal{L}\{\rho\}$$

$$\mathcal{L}\{\rho\} = -\Gamma \begin{pmatrix} (\rho_L - \rho_L^0) & \frac{1}{2}\rho_{LEM} & \rho_{LR} \\ \frac{1}{2}\rho_{EM,L} & 0_{EM} & \frac{1}{2}\rho_{EM,R} \\ \rho_{RL} & \frac{1}{2}\rho_{REM} & (\rho_R - \rho_R^0) \end{pmatrix}$$

■ INTRODUCTION

Since its inception over 40 years ago¹ the field of molecular electronics has held the promise to use individual molecular entities and their assemblies as active components in electronic devices.^{2–4} Molecules are often characterized by their miniature size, quantum-mechanical nature, well-defined chemical composition, highly efficient and accurate synthesis procedures, as well as self-assembly capabilities. These properties open the door for the design of novel molecular-scale electronic components that may present unique functionality with high sensitivity toward external perturbations and fast response time. Furthermore, such systems are expected to be energetically efficient and to allow for cost-effective reproducible device fabrication.

Steady-state transport properties of molecular junctions remain the main focus of both experimental and theoretical efforts in this field. Nevertheless, the study of dynamical transport phenomena in nanoscale junctions has recently gained increasing attention from the scientific community.^{5–32} Research in this direction explores the effects of time-dependent perturbations such as alternating currents, bias pulses, and external electromagnetic fields on the transient response of the system. This involves complex physical processes that can be harnessed for the design of miniaturized electronic devices such as optoelectronic ultrafast molecular switches and nanoscale rectifiers.^{7,8,14,22,24–27,29,31}

Considering the temporal degree of freedom poses new challenges on the experimental efforts that theory and simulation may help resolve via the prediction of optimal junction configurations and operation conditions and the interpretation of experimental findings. To this end, various methods aiming to simulate electron dynamics in molecular junctions have been developed.^{31–90} These approaches either consider the detailed atomistic structure of the junction or introduce model Hamiltonians to study specific transport

phenomena. Furthermore, they vary in the level of treatment of electron–electron interactions and effects of bath memory.

Recently, we proposed the Driven Liouville von Neumann approach that imposes dynamic nonequilibrium boundary conditions on finite atomistic models of realistic molecular junctions.^{91,92} This method was shown to provide a decent compromise between computational efficiency and physical accuracy when modeling single-electron dynamics in molecular junctions subjected to time-dependent external perturbations.⁹³ Notably, the underlying equation of motion was numerically shown to solve the density matrix positivity conservation violation found in previous related implementations.⁸⁰ This gained further formal support when the equation was explicitly derived as an approximate form of nonequilibrium Green's function formalism.⁹³ Nevertheless, no direct rigorous proof was offered to support the general validity of the positivity condition for this method. In the present study, we show that in the limit of infinite lead models the Driven Liouville von Neumann equation can be written in Lindblad form. The latter guarantees preservation of density matrix positivity^{94–96} as well as N -representability of the N -electron density matrix and, under certain conditions, also of the one-electron reduced density matrix⁹⁷ throughout the dynamics thus justifying the numerical findings.

■ DERIVATION

Consider the system depicted in Figure 1. Here a molecule bridges the gap between two leads that are connected to two external baths. We formally divide the system into five sections including the left and right semi-infinite reservoirs, the left and

Special Issue: Ronnie Kosloff Festschrift

Received: December 14, 2015

Revised: January 22, 2016

Published: January 25, 2016

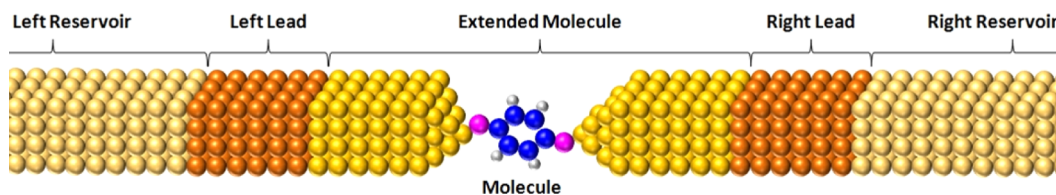


Figure 1. Real-space representation of a typical molecular junction model divided into the extended molecule, left and right leads, and external reservoirs.

right leads, and the extended molecule region, which is the molecule itself augmented by its adjacent lead sections. The size of these lead sections is chosen such that the electronic properties of the full extended molecule converge to within a desired accuracy. In the present derivation we do not treat the reservoirs explicitly and instead we take them into account implicitly by considering their effect on their adjacent lead sections. So, in practice, we consider a system constructed from the finite left and right lead models connected by the extended molecule. The corresponding sets of orthonormal eigenstates of each individual section are marked as $\{|l\rangle\}$, $\{|r\rangle\}$, and $\{|m\rangle\}$, respectively.

We aim at showing that the driven Liouville von Neumann equation that was previously derived both heuristically⁹¹ and explicitly⁹³ can be written in Lindblad form, thus proving that the corresponding nonunitary evolution of the density matrix is indeed completely positive. To this end, we start from the Lindblad super operator that has the following general form

$$\mathcal{L}\{\hat{\rho}\} = \sum_{\alpha} \left[\hat{L}_{\alpha} \hat{\rho} \hat{L}_{\alpha}^{\dagger} - \frac{1}{2} \hat{L}_{\alpha}^{\dagger} \hat{L}_{\alpha} \hat{\rho} - \frac{1}{2} \hat{\rho} \hat{L}_{\alpha}^{\dagger} \hat{L}_{\alpha} \right] \quad (1)$$

where $\hat{\rho}$ is the density operator and \hat{L}_{α} are Lindblad operators that we choose in the form previously suggested by Dubi and Di Ventra⁹⁸

$$\hat{L}_{k,k'} = \sqrt{\gamma_{k,k} f_K(E_k, \mu_K)} |k\rangle \langle k'| \quad (2)$$

Here $|k\rangle \in \{|l\rangle\}$ or $\{|r\rangle\}$ are single-particle states in the left ($K = L$) or right ($K = R$) noninteracting lead sections, respectively. The action of these operators is to exchange charge between each finite lead model levels with (real) transition rates $\{\gamma_{k,k'}\}$ so as to maintain, as close as possible, their Fermi–Dirac equilibrium distribution $f_K(E, \mu_K) = [1 + e^{(E - \mu_K)/(k_B T_K)}]^{-1}$ induced by their implicit coupling to the corresponding reservoirs. Here, T_K and μ_K are the electronic temperature and chemical potential of reservoir K and k_B is Boltzmann's constant. With this choice the Lindblad superoperator can be split into the individual contributions of the left and right leads $\mathcal{L}\{\hat{\rho}\} = \mathcal{L}_L\{\hat{\rho}\} + \mathcal{L}_R\{\hat{\rho}\}$ with

$$\mathcal{L}_K\{\hat{\rho}\} = \sum_{k=1}^{N_K} \sum_{k'=1, k' \neq k}^{N_K} \left[\hat{L}_{k,k'} \hat{\rho} \hat{L}_{k,k'}^{\dagger} - \frac{1}{2} \hat{L}_{k,k'}^{\dagger} \hat{L}_{k,k'} \hat{\rho} - \frac{1}{2} \hat{\rho} \hat{L}_{k,k'}^{\dagger} \hat{L}_{k,k'} \right] \quad (3)$$

where the sums run over all N_K levels of lead K with $k' \neq k$. To obtain the driven Liouville von Neumann equation we write this superoperator in matrix form. Using eq 2, the first term in the double sum can be written as

$$\begin{aligned} \hat{L}_{k,k'} \hat{\rho} \hat{L}_{k,k'}^{\dagger} &= \left[\sqrt{\gamma_{k,k} f_K(E_k, \mu_K)} |k\rangle \langle k'| \right] \hat{\rho} \left[\langle k'| \right. \\ &\quad \left. \sqrt{\gamma_{k,k} f_K(E_k, \mu_K)} \right] \\ &= \gamma_{k,k} f_K(E_k, \mu_K) \rho_{k',k} |k\rangle \langle k| \end{aligned} \quad (4)$$

where we have denoted the matrix element $\rho_{k',k} \equiv \langle k'| \hat{\rho} |k\rangle$. The second term is given by

$$\begin{aligned} -\frac{1}{2} \hat{L}_{k,k}^{\dagger} \hat{L}_{k,k} \hat{\rho} &= -\frac{1}{2} \left[\sqrt{\gamma_{k,k} f_K(E_k, \mu_K)} |k\rangle \langle k| \right] \left[|k\rangle \langle k'| \right. \\ &\quad \left. \sqrt{\gamma_{k,k} f_K(E_k, \mu_K)} \right] \hat{\rho} \\ &= -\frac{1}{2} \gamma_{k,k} f_K(E_k, \mu_K) |k\rangle \langle k'| \hat{\rho} \\ &= -\frac{1}{2} \gamma_{k,k} f_K(E_k, \mu_K) \sum_{n \in \{|l\rangle\}, \{|m\rangle\}, \{|r\rangle\}} \rho_{k',n} |k\rangle \langle n| \end{aligned} \quad (5)$$

where we introduced the identity operator within the subspace of system states: $\hat{I} = \sum_{n \in \{|l\rangle\}, \{|m\rangle\}, \{|r\rangle\}} |n\rangle \langle n|$. Accordingly, the third term can be written as

$$-\frac{1}{2} \hat{\rho} \hat{L}_{k,k}^{\dagger} \hat{L}_{k,k} = -\frac{1}{2} \gamma_{k,k} f_K(E_k, \mu_K) \sum_{n \in \{|l\rangle\}, \{|m\rangle\}, \{|r\rangle\}} \rho_{n,k} |n\rangle \langle k'| \quad (6)$$

Substituting eqs 4–6 in eq 3 we obtain an expression for the Lindblad superoperator of lead K

$$\begin{aligned} \mathcal{L}_K\{\hat{\rho}\} &= \sum_{k=1}^{N_K} \sum_{k'=1}^{N_K} \gamma_{k,k'} f_K(E_k, \mu_K) \left[\rho_{k',k} |k\rangle \langle k| \right. \\ &\quad \left. - \frac{1}{2} \sum_{n \in \{|l\rangle\}, \{|m\rangle\}, \{|r\rangle\}} (\rho_{k',n} |k\rangle \langle n| + \rho_{n,k} |n\rangle \langle k'|) \right] \\ &\quad - \sum_{k=1}^{N_K} \gamma_{k,k} f_K(E_k, \mu_K) \left[\rho_{k,k} |k\rangle \langle k| \right. \\ &\quad \left. - \frac{1}{2} \sum_{n \in \{|l\rangle\}, \{|m\rangle\}, \{|r\rangle\}} (\rho_{k,n} |k\rangle \langle n| + \rho_{n,k} |n\rangle \langle k|) \right] \end{aligned} \quad (7)$$

where we have added and subtracted the terms with $k' = k$. The eigenstates of each section ($\{|l\rangle\}$, $\{|m\rangle\}$, $\{|r\rangle\}$) form an orthogonal set within themselves by construction. Furthermore, assuming a tight-binding approximation, the overlap between states of different sections is neglected, thus making them mutually orthogonal. Therefore, the diagonal elements of the matrix representation of $\mathcal{L}_K\{\hat{\rho}\}$ are given by

$$\begin{aligned}
\langle i|\mathcal{L}_K|i\rangle = & \sum_{k=1}^{N_K} \sum_{k'=1}^{N_K} \gamma_{k,k'} f_K(E_k, \mu_K) \left[\rho_{k',k'} \delta_{ik} \delta_{ki} \right. \\
& - \frac{1}{2} \sum_{n \in \{\ell\}, \{m\}, \{r\}} (\rho_{k',n} \delta_{ik} \delta_{ni} + \rho_{n,k'} \delta_{im} \delta_{k'i}) \\
& - \sum_{k=1}^{N_K} \gamma_{k,k} f_K(E_k, \mu_K) \left[\rho_{k,k} \delta_{ik} \delta_{ki} \right. \\
& \left. \left. - \frac{1}{2} \sum_{n \in \{\ell\}, \{m\}, \{r\}} (\rho_{k,n} \delta_{ik} \delta_{ni} + \rho_{n,k} \delta_{im} \delta_{ki}) \right] \right] \quad (8)
\end{aligned}$$

Clearly, if $|i\rangle$ does not belong to the set of eigenstates $\{|k\rangle\}$ of lead K this term completely vanishes, whereas when $|i\rangle \in \{|k\rangle\}$ the second sum vanishes and the only terms that survive are

$$\langle i|\mathcal{L}_K|i\rangle = \sum_{k=1}^{N_K} \gamma_{i,k} f_K(E_i, \mu_K) \rho_{k,k} - \sum_{k=1}^{N_K} \gamma_{k,i} f_K(E_k, \mu_K) \rho_{i,i} \quad (9)$$

where, for brevity, we have replaced the summation index k' by k in the first sum.

For the off-diagonal matrix elements of $\mathcal{L}_K\{\hat{\rho}\}$ we obtain

$$\begin{aligned}
\langle i|\mathcal{L}_K|j \neq i\rangle & = -\frac{1}{2} \sum_{k=1}^{N_K} \sum_{k'=1}^{N_K} \gamma_{k,k'} f_K(E_k, \mu_K) \\
& \sum_{n \in \{\ell\}, \{m\}, \{r\}} (\rho_{k',n} \delta_{ik} \delta_{nj} + \rho_{n,k'} \delta_{im} \delta_{k'j}) \\
& + \frac{1}{2} \sum_{k=1}^{N_K} \gamma_{k,k} f_K(E_k, \mu_K) \sum_{n \in \{\ell\}, \{m\}, \{r\}} (\rho_{k,n} \delta_{ik} \delta_{nj} \\
& + \rho_{n,k} \delta_{im} \delta_{kj}) \quad (10)
\end{aligned}$$

where terms involving $\delta_{ik} \delta_{kj}$ have been omitted. When $|i\rangle, |j\rangle \in \{|k\rangle\}$ this expression yields

$$\begin{aligned}
\langle i|\mathcal{L}_K|j\rangle & = \frac{1}{2} [\gamma_{i,i} f_K(E_i, \mu_K) + \gamma_{j,j} f_K(E_j, \mu_K) \\
& - \sum_{k=1}^{N_K} (\gamma_{k,i} + \gamma_{k,j}) f_K(E_k, \mu_K)] \rho_{i,j} \quad (11)
\end{aligned}$$

For $|i\rangle \in \{|k\rangle\}$ and $|j\rangle \notin \{|k\rangle\}$ this term gives

$$\langle i|\mathcal{L}_K|j\rangle = -\frac{1}{2} \left[\sum_{k \neq i} \gamma_{k,i} f_K(E_k, \mu_K) \right] \rho_{i,j} \quad (12)$$

Similarly, for $|i\rangle \notin \{|k\rangle\}$ and $|j\rangle \in \{|k\rangle\}$ we obtain

$$\langle i|\mathcal{L}_K|j\rangle = -\frac{1}{2} \left[\sum_{k \neq j} \gamma_{k,j} f_K(E_k, \mu_K) \right] \rho_{i,j} \quad (13)$$

and when $|i\rangle, |j\rangle \notin \{|k\rangle\}$

$$\langle i|\mathcal{L}_K|j\rangle = 0 \quad (14)$$

Collecting all of the terms appearing in eqs 9 and 11–14 we obtain the following expression for the matrix elements of the Lindblad super operator defined by eqs 2 and 3 on the basis of

single-particle states of the separate system sections (left and right leads and the extended molecule)

$$\langle i|\mathcal{L}_K|j\rangle = \begin{cases} \sum_{k=1}^{N_K} \gamma_{i,k} f_K(E_i, \mu_K) \rho_{k,k} & i = j; |i\rangle, |j\rangle \in \{|k\rangle\} \\ - \sum_{k=1}^{N_K} \gamma_{k,i} f_K(E_k, \mu_K) \rho_{i,i} & \\ 0 & i = j; |i\rangle, |j\rangle \notin \{|k\rangle\} \\ \frac{1}{2} \left[\gamma_{i,i} f_K(E_i, \mu_K) + \gamma_{j,j} f_K(E_j, \mu_K) \right. \\ \left. - \sum_{k=1}^{N_K} (\gamma_{k,i} + \gamma_{k,j}) \right. \\ \left. f_K(E_k, \mu_K) \right] \rho_{i,j} & i \neq j; |i\rangle, |j\rangle \in \{|k\rangle\} \\ - \frac{1}{2} \left[\sum_{k \neq i} \gamma_{k,i} f_K(E_k, \mu_K) \right] \rho_{i,j} & i \neq j; |i\rangle \in \{|k\rangle\}, |j\rangle \notin \{|k\rangle\} \\ - \frac{1}{2} \left[\sum_{k \neq j} \gamma_{k,j} f_K(E_k, \mu_K) \right] \rho_{i,j} & i \neq j; |i\rangle \notin \{|k\rangle\}, |j\rangle \in \{|k\rangle\} \\ 0 & i \neq j; |i\rangle, |j\rangle \notin \{|k\rangle\} \end{cases} \quad (15)$$

At this point we assume that all interstate transition rates are equal and constant such that $\gamma_{k,k'} = \gamma_K = \text{Const}$ giving

$$\langle i|\mathcal{L}_K|j\rangle = \gamma_K \begin{cases} f_K(E_i, \mu_K) \sum_{k=1}^{N_K} \rho_{k,k} & i = j; |i\rangle, |j\rangle \in \{|k\rangle\} \\ - \left[\sum_{k=1}^{N_K} f_K(E_k, \mu_K) \right] \rho_{i,i} & \\ 0 & i = j; |i\rangle, |j\rangle \notin \{|k\rangle\} \\ \frac{1}{2} \left[f_K(E_i, \mu_K) + f_K(E_j, \mu_K) \right. \\ \left. - 2 \sum_{k=1}^{N_K} f_K(E_k, \mu_K) \right] \rho_{i,j} & i \neq j; |i\rangle, |j\rangle \in \{|k\rangle\} \\ - \frac{1}{2} \left[\sum_{k \neq i} f_K(E_k, \mu_K) \right] \rho_{i,j} & i \neq j; |i\rangle \in \{|k\rangle\}, |j\rangle \notin \{|k\rangle\} \\ - \frac{1}{2} \left[\sum_{k \neq j} f_K(E_k, \mu_K) \right] \rho_{i,j} & i \neq j; |i\rangle \notin \{|k\rangle\}, |j\rangle \in \{|k\rangle\} \\ 0 & i \neq j; |i\rangle, |j\rangle \notin \{|k\rangle\} \end{cases} \quad (16)$$

The partial trace of the density matrix over the states of lead K appearing in the expression for the nonzero diagonal terms in eq 16 provides the instantaneous number of electrons in the finite lead model $\sum_{k=1}^{N_K} \rho_{k,k} = N_K$. Similarly, the sum over Fermi–Dirac weights results in the corresponding equilibrium number of electrons $\sum_{k=1}^{N_K} f_K(E_k, \mu_K) = N_K^{\text{Eq}}$. Hence, for $i \in \{|k\rangle\}$ we obtain

$$\begin{aligned}
\langle i|\mathcal{L}_K|i\rangle & = \gamma_K [f_K(E_i, \mu_K) N_K - N_K^{\text{Eq}} \rho_{i,i}] \\
& = \gamma_K N_K^{\text{Eq}} \left[f_K(E_i, \mu_K) \frac{N_K}{N_K^{\text{Eq}}} - \rho_{i,i} \right] \quad (17)
\end{aligned}$$

In the limit of infinite lead models the effect of the extended molecule on the leads becomes negligible and the Lindblad

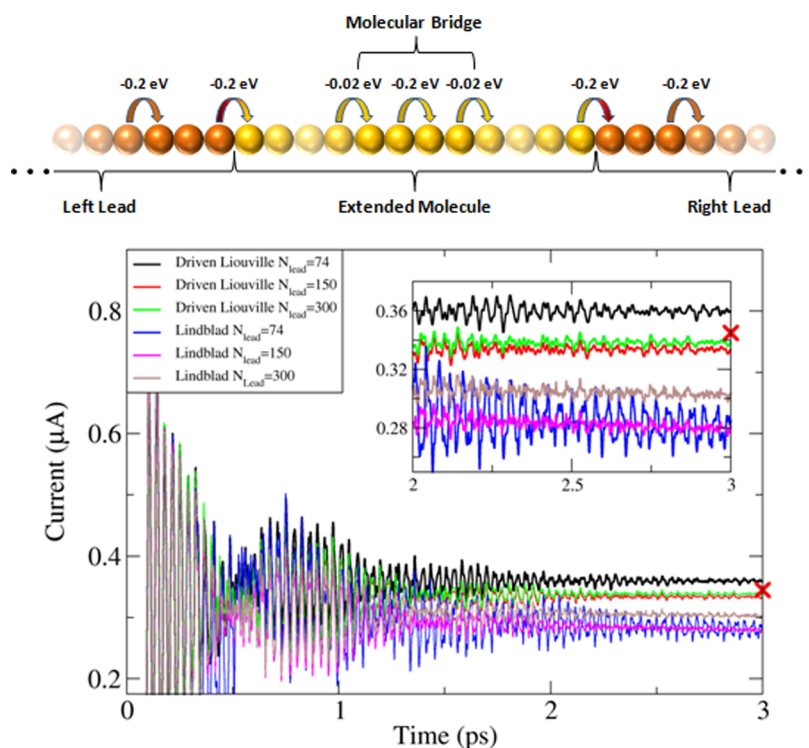


Figure 2. Current versus time of a tight-binding atomic chain calculated using the driven Liouville von Neumann equation (black, red, and green) and the Lindblad equation (blue, violet, and brown). Three different lead model sizes with increasing length of 74 (black and blue), 150 (red and violet), and 300 (green and brown) sites are considered. The Landauer steady-state value is presented for reference as the red \times . The extended molecule length is 110 sites with 10 sites representing the molecular bridge and 50 sites on each of the bridge sides to represent the lead sections within the extended molecule region. All onsite energies are set to zero, the hopping integrals within the left, right, and extended molecule sections are taken to be -0.2 eV, and the hopping integral between the two edge sites of the molecular bridge and the corresponding edge sites of the lead sections in the extended molecule is taken as -0.02 eV (see illustration above the diagram). The bias voltage considered is 0.2 V and the lead electronic temperatures are set to 0 K. The inset provides a zoom-in on the steady-state transport region.

operators of eq 2 drive the lead occupations toward their equilibrium state such that $\frac{N_k}{N_k^{\text{Eq}}} \rightarrow 1$, and thus we obtain

$$\langle i|\mathcal{L}_L|i\rangle \xrightarrow{N_K \rightarrow \infty} \gamma_K N_K^{\text{Eq}} [f_K(E_i, \mu_K) - \rho_{i,i}] \quad (18)$$

Accordingly, for the off-diagonal terms with $|i\rangle, |j\rangle \in \{|k\rangle\}$ we have

$$\langle i|\mathcal{L}_K|j\rangle = \frac{\gamma_K N_K^{\text{Eq}}}{2} \left[\frac{f_K(E_i, \mu_K) + f_K(E_j, \mu_K)}{N_K^{\text{Eq}}} - 2 \right] \rho_{i,j} \quad (19)$$

Because $f_K(E_i, \mu_K)$ and $f_K(E_j, \mu_K)$ are both positive fractions, in the limit of infinite lead models the first term in the square brackets in eq 19 vanishes, leaving

$$\langle i|\mathcal{L}_K|j\rangle \xrightarrow{N_K^{\text{Eq}} \rightarrow \infty} -\gamma_K N_K^{\text{Eq}} \rho_{i,j} \quad (20)$$

The remaining nonzero off-diagonal terms of \mathcal{L}_K have either the form

$$\begin{aligned} \langle i|\mathcal{L}_K|j\rangle &= -\frac{\gamma_K}{2} \left[\sum_{k \neq i}^{N_K} f_K(E_k, \mu_K) \right] \rho_{i,j} \\ &= -\frac{\gamma_K}{2} \left[\sum_{k=1}^{N_K} f_K(E_k, \mu_K) - f_K(E_i, \mu_K) \right] \rho_{i,j} \\ &= -\frac{\gamma_K}{2} [N_K^{\text{Eq}} - f_K(E_i, \mu_K)] \rho_{i,j} \\ &= -\frac{\gamma_K N_K^{\text{Eq}}}{2} \left[1 - \frac{f_K(E_i, \mu_K)}{N_K^{\text{Eq}}} \right] \rho_{i,j} \xrightarrow{N_K^{\text{Eq}} \rightarrow \infty} -\frac{\gamma_K N_K^{\text{Eq}}}{2} \rho_{i,j} \end{aligned} \quad (21)$$

when $i \in \{|k\rangle\}, j \notin \{|k\rangle\}$ or

$$\langle i|\mathcal{L}_K|j\rangle = -\frac{\gamma_K N_K^{\text{Eq}}}{2} \left[1 - \frac{f_K(E_j, \mu_K)}{N_K^{\text{Eq}}} \right] \rho_{i,j} \xrightarrow{N_K^{\text{Eq}} \rightarrow \infty} -\frac{\gamma_K N_K^{\text{Eq}}}{2} \rho_{i,j} \quad (22)$$

when $i \notin \{|k\rangle\}, j \in \{|k\rangle\}$, thus yielding the same expression.

Collecting all terms appearing in eqs 18 and 20–22 and substituting in eq 16, we finally obtain

$$\langle i|\mathcal{L}_K|j\rangle = -\gamma_K N_K^{\text{eq}} \begin{cases} [\rho_{i,i} - f_K(E_i, \mu_K)] & i = j; |i\rangle, |j\rangle \in \{|k\rangle\} \\ \rho_{i,j} & i \neq j; |i\rangle, |j\rangle \in \{|k\rangle\} \\ \frac{1}{2}\rho_{i,j} & i \neq j; |i\rangle \in \{|k\rangle\}, |j\rangle \notin \{|k\rangle\} \\ \frac{1}{2}\rho_{i,j} & i \neq j; |i\rangle \notin \{|k\rangle\}, |j\rangle \in \{|k\rangle\} \\ 0 & \text{otherwise} \end{cases} \quad (23)$$

In matrix form the Lindblad superoperator is thus given by

$$\mathcal{L}\{\rho\} = \mathcal{L}_L\{\rho\} + \mathcal{L}_R\{\rho\} = \begin{pmatrix} -\Gamma_L(\rho_L - \rho_L^0) & -\frac{\Gamma_L}{2}\rho_{L,EM} & -\left(\frac{\Gamma_L}{2} + \frac{\Gamma_R}{2}\right)\rho_{L,R} \\ -\frac{\Gamma_L}{2}\rho_{EM,L} & \mathbf{0}_M & -\frac{\Gamma_R}{2}\rho_{EM,R} \\ -\left(\frac{\Gamma_L}{2} + \frac{\Gamma_R}{2}\right)\rho_{R,L} & -\frac{\Gamma_R}{2}\rho_{R,EM} & -\Gamma_R(\rho_R - \rho_R^0) \end{pmatrix} \quad (24)$$

where we have defined $\rho_K^0 \equiv \text{diag}\{f_K(E_k, \mu_K)\}$ as a diagonal matrix of dimensions $K \times K$, whose k th diagonal element is given by $f_K(E_k, \mu_K)$ and $\Gamma_K \equiv \gamma_K N_K^{\text{eq}}$. If we further assume that $\Gamma_L = \Gamma_R \equiv \Gamma$, eq 24 reduces to

$$\mathcal{L}\{\rho\} = -\Gamma \begin{pmatrix} (\rho_L - \rho_L^0) & \frac{1}{2}\rho_{L,EM} & \rho_{L,R} \\ \frac{1}{2}\rho_{EM,L} & \mathbf{0}_M & \frac{1}{2}\rho_{EM,R} \\ \rho_{R,L} & \frac{1}{2}\rho_{R,EM} & (\rho_R - \rho_R^0) \end{pmatrix} \quad (25)$$

which has the exact same structure as the driving term of the driven Liouville von Neumann equation,^{91–93} thus completing the derivation.

NUMERICAL DEMONSTRATION

To demonstrate the correspondence between the Lindblad superoperator defined by eqs 1 and 2 and the driving term appearing in eq 25, we used both to perform comparative numerical simulations of the electronic transport through a tight-binding atomic chain with increasing lead models size. To this end, we propagate the quantum master equation

$$\dot{\rho}(t) = -\frac{i}{\hbar}[\mathbf{H}, \rho] + \mathcal{L}\{\rho\} \quad (26)$$

where the matrix elements of the superoperator \mathcal{L} are given by either eq 16 or eq 25. Figure 2 compares the time-dependent current obtained by the two methods for increasing lead model systems.⁹⁹ The model parameters are detailed in the Figure caption. Constant driving rates of $\gamma_L = \gamma_R = \gamma = 1 \times 10^{-4} \text{ fs}^{-1}$ are used in all Lindblad equation calculations, and the corresponding driving rate used for the driven Liouville von Neumann equation calculations is $\Gamma = 0.015 \text{ fs}^{-1}$. The two values are related via $\Gamma \equiv \gamma N^{\text{eq}}$ for the 150 sites lead model system where the average lead equilibrium occupation is $N^{\text{eq}} = 150$. As can be seen, the results of the driven Liouville von Neumann calculations quickly converge with lead size such that already for a lead of 150 sites good agreement is obtained with

the Landauer steady-state current value. The Lindblad currents, which are consistently smaller than the Driven Liouville von Neumann results, gradually approach the correct steady-state value and the Driven Liouville von Neumann current traces with increasing lead size. This indicates that indeed at sufficiently large lead models the methods become equivalent. Nevertheless, even at a lead size of 300 sites the Lindblad results are not fully converged and deviate from the Landauer value.

To better understand this behavior we analyze the steady-state populations as obtained by the two methods with increasing lead size. In Figure 3a we present the lead and

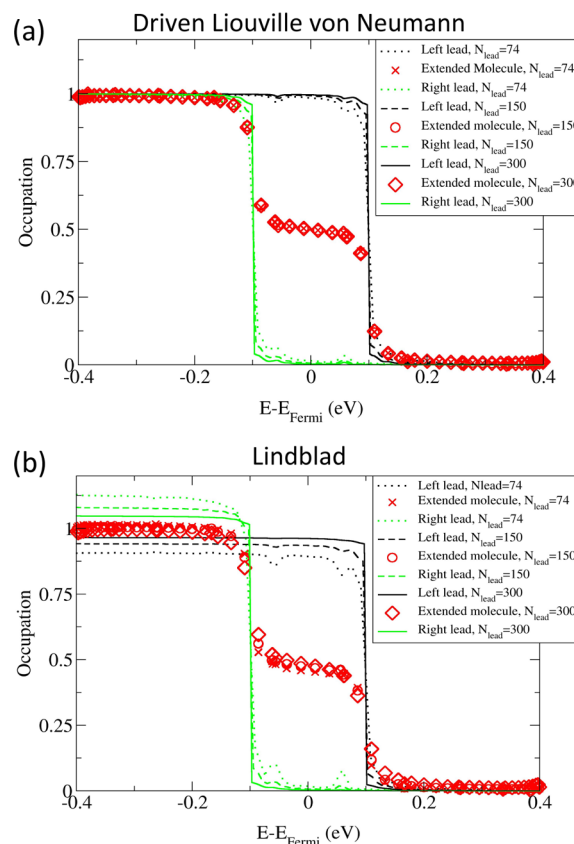


Figure 3. Steady-state occupations of the left lead (black), extended molecule (red), and right lead (green) single-particle states as obtained using the driven Liouville von Neumann (a) and the Lindblad (b) master equations for increasing lead sizes of 74 (dotted lines), 150 (dashed lines), and 300 (full lines) sites. The model parameters are detailed in the caption of Figure 2.

extended molecule-state occupations obtained at steady-state using the Driven Liouville von Neumann equation of motion for the three tight-binding chain lead sizes. Notably, all populations are between 0 and 1, indicating that N representability is conserved. Furthermore, the molecular occupations are converged already for the shortest lead model considered of 74 sites, while the lead occupation deviations from the target equilibrium distribution reduce with increasing lead size.

The corresponding results for the Lindblad equation are presented in Figure 3b. As may be expected, all state occupations are positive. Nevertheless, large deviations of the lead steady-state occupations from the target Fermi–Dirac distributions appear. These are characterized by clear violations

of the N -representability condition leading to occupations that exceed one particle per state in disagreement with Pauli's exclusion principle.⁹⁷ The deviations reduce with increasing lead size but are still quite significant, even at a lead model size of 300 sites. Accordingly, the extended molecule steady-state occupations, that resemble those obtained by the driven Liouville von Neumann approach, are not fully converged at this lead size. These results further indicate the robustness of the driven Liouville von Neumann equation for describing time-dependent transport in molecular junctions.

It is important to note that in order to provide an appropriate comparison between the driven Liouville von Neumann and the Lindblad equations we restrict the calculation to a single driving rate applied uniformly to all lead model eigenstates. Reference 98 provides a scheme to calculate state-dependent transition rates within the Lindblad formalism. These may reduce deviations from N -representability conservation and improve convergence of the Lindblad calculation. In fact, the reason that a single driving rate description works well for the driven Liouville von Neumann approach within the tight-binding Hamiltonian is the uniform density of states of the finite lead models. From an energy perspective, the driving parameter serves to broaden the lead eigenstates so as to obtain a continuous spectrum as required from any descent lead model. When the lead density of states is uniform, a single broadening factor is sufficient to achieve this goal. For more advanced Hamiltonian models, such as those obtained within nonorthogonal basis set representations, that produce a nonuniform density of states, the single driving rate description is insufficient and more advanced schemes to calculate state-dependent broadening factors are required. This, indeed, is a subject of current research.

SUMMARY AND CONCLUSIONS

We have shown that in the limit of infinite lead model size the driven Liouville von Neumann equation of motion can be written in Lindblad form. This rationalizes the numerical observation of density matrix positivity conservation exhibited by this equation. Furthermore, it establishes a link between the exact equation of motion, to which the driven Liouville von Neumann equation was shown to be an approximation,⁹³ and the Lindblad operators adopted herein.

AUTHOR INFORMATION

Corresponding Author

*E-mail: odedhod@tau.ac.il

Notes

The authors declare no competing financial interest.

ACKNOWLEDGMENTS

O.H. thanks Prof. Leeor Kronik, Dr. Yonatan Dubi, and Dr. Felipe Barra for insightful discussions on the subject. Work at TAU was supported by the German-Israeli Foundation under research grant no. 2291-2259.5/2011, the Israel Science Foundation under grant no. 1740/13, the Raymond and Beverly Sackler Fund for Convergence Research in Biomedical, Physical and Engineering Sciences, the Lise-Meitner Minerva Center for Computational Quantum Chemistry, and the Center for Nanoscience and Nanotechnology at Tel-Aviv University.

REFERENCES

- (1) Aviram, A.; Ratner, M. A. Molecular Rectifiers. *Chem. Phys. Lett.* **1974**, *29*, 277–283.
- (2) Aradhya, S. V.; Venkataraman, L. Single-Molecule Junctions Beyond Electronic Transport. *Nat. Nanotechnol.* **2013**, *8*, 399–410.
- (3) Bergfield, J. P.; Ratner, M. A. Forty Years of Molecular Electronics: Non-Equilibrium Heat and Charge Transport at the Nanoscale. *Phys. Status Solidi B* **2013**, *250*, 2249–2266.
- (4) Ghosh, A. W.; Damle, P. S.; Datta, S.; Nitzan, A. Molecular Electronics: Theory and Device Prospects. *MRS Bull.* **2004**, *29*, 391–395.
- (5) Kohler, S.; Lehmann, J.; Camalet, S.; Hänggi, P. Resonant Laser Excitation of Molecular Wires. *Isr. J. Chem.* **2002**, *42*, 135–141.
- (6) Tikhonov, A.; Coalson, R. D.; Dahnovsky, Y. Calculating Electron Current in a Tight-Binding Model of a Field-Driven Molecular Wire: Application to Xylyl-dithiol. *J. Chem. Phys.* **2002**, *117*, 567–580.
- (7) Lehmann, J.; Kohler, S.; Hänggi, P.; Nitzan, A. Molecular Wires Acting as Coherent Quantum Ratchets. *Phys. Rev. Lett.* **2002**, *88*, 228305.
- (8) Lehmann, J.; Kohler, S.; Hänggi, P.; Nitzan, A. Rectification of Laser-Induced Electronic Transport Through Molecules. *J. Chem. Phys.* **2003**, *118*, 3283–3293.
- (9) Camalet, S.; Lehmann, J.; Kohler, S.; Hänggi, P. Current Noise in ac-Driven Nanoscale Conductors. *Phys. Rev. Lett.* **2003**, *90*, 210602.
- (10) Kohler, S.; Lehmann, J.; Strass, M.; Hänggi, P. Molecular Wires in Electromagnetic Fields. In *Adv. Solid State Phys.*; Kramer, B., Ed.; Advances in Solid State Physics; Springer: Berlin Heidelberg, 2004; Vol. 44; pp 157–167.
- (11) Ovchinnikov, I. V.; Neuhauser, D. A Liouville Equation for Systems which Exchange Particles with Reservoirs: Transport Through a Nanodevice. *J. Chem. Phys.* **2005**, *122*, 024707.
- (12) Kaun, C.-C.; Seideman, T. Current-Driven Oscillations and Time-Dependent Transport in Nanojunctions. *Phys. Rev. Lett.* **2005**, *94*, 226801.
- (13) Hänggi, P.; Kohler, S.; Lehmann, J.; Strass, M. AC-Driven Transport Through Molecular Wires. In *Introducing Molecular Electronics*; Cuniberti, G.; Fagas, G.; Richter, K., Eds.; Springer-Verlag, New York, 2005; Vol. 680; pp 55–75.
- (14) Galperin, M.; Nitzan, A. Current-Induced Light Emission and Light-Induced Current in Molecular-Tunneling Junctions. *Phys. Rev. Lett.* **2005**, *95*, 206802.
- (15) Kohler, S.; Lehmann, J.; Hänggi, P. Driven Quantum Transport on the Nanoscale. *Phys. Rep.* **2005**, *406*, 379–443.
- (16) Kleinekathöfer, U.; Li, G. Q.; Welack, S.; Schreiber, M. Coherent Destruction of the Current Through Molecular Wires Using Short Laser Pulses. *Phys. Status Solidi B* **2006**, *243*, 3775–3781.
- (17) Kleinekathöfer, U.; Guangqi, L.; Welack, S.; Schreiber, M. Switching the Current Through Model Molecular Wires with Gaussian Laser Pulses. *Europhys. Lett.* **2006**, *75*, 139–145.
- (18) Welack, S.; Schreiber, M.; Kleinekathöfer, U. The Influence of Ultrafast Laser Pulses on Electron Transfer in Molecular Wires Studied by a non-Markovian Density-Matrix Approach. *J. Chem. Phys.* **2006**, *124*, 044712.
- (19) Li, G. Q.; Schreiber, M.; Kleinekathöfer, U. Coherent Laser Control of the Current Through Molecular Junctions. *Eur. Phys. Lett.* **2007**, *79*, 27006.
- (20) Galperin, M.; Ratner, M. A.; Nitzan, A. Molecular Transport Junctions: Vibrational Effects. *J. Phys.: Condens. Matter* **2007**, *19*, 103201.
- (21) Fainberg, B. D.; Jouravlev, M.; Nitzan, A. Light-Induced Current in Molecular Tunneling Junctions Excited with Intense Shaped Pulses. *Phys. Rev. B: Condens. Matter Mater. Phys.* **2007**, *76*, 245329.
- (22) Kohler, S.; Hänggi, P. Molecular Electronics: Ultrafast Stop and Go. *Nat. Nanotechnol.* **2007**, *2*, 675–676.
- (23) Li, G.; Welack, S.; Schreiber, M.; Kleinekathöfer, U. Tailoring Current Flow Patterns Through Molecular Wires Using Shaped Optical Pulses. *Phys. Rev. B: Condens. Matter Mater. Phys.* **2008**, *77*, 075321.

- (24) Franco, I.; Shapiro, M.; Brumer, P. Laser-Induced Currents Along Molecular Wire Junctions. *J. Chem. Phys.* **2008**, *128*, 244906.
- (25) Fainberg, B. D.; Hanggi, P.; Kohler, S.; Nitzan, A.; Singh, M. R.; Lipson, R. H. Exciton- and Light-Induced Current in Molecular Nanojunctions. *Am. Inst. Phys. Conf. Proc.* **2009**, *1147*, 78–86.
- (26) Jorn, R.; Seideman, T. Competition Between Current-Induced Excitation and Bath-Induced Decoherence in Molecular Junctions. *J. Chem. Phys.* **2009**, *131*, 244114.
- (27) Volkovich, R.; Peskin, U. Transient Dynamics in Molecular Junctions: Coherent Bichromophoric Molecular Electron Pumps. *Phys. Rev. B: Condens. Matter Mater. Phys.* **2011**, *83*, 033403.
- (28) Renaud, N.; Ratner, M. A.; Joachim, C. A Time-Dependent Approach to Electronic Transmission in Model Molecular Junctions. *J. Phys. Chem. B* **2011**, *115*, 5582–5592.
- (29) Peskin, U.; Galperin, M. Coherently Controlled Molecular Junctions. *J. Chem. Phys.* **2012**, *136*, 044107.
- (30) Galperin, M.; Nitzan, A. Molecular Optoelectronics: the Interaction of Molecular Conduction Junctions with Light. *Phys. Chem. Chem. Phys.* **2012**, *14*, 9421–9438.
- (31) Selzer, Y.; Peskin, U. Transient Dynamics in Molecular Junctions: Picosecond Resolution from dc Measurements by a Laser Pulse Pair Sequence Excitation. *J. Phys. Chem. C* **2013**, *117*, 22369–22376.
- (32) Ke, S.; Liu, R.; Yang, W.; Baranger, H. U. Time-Dependent Transport Through Molecular Junctions. *J. Chem. Phys.* **2010**, *132*, 234105.
- (33) Stefanucci, G.; Almbladh, C.-O. Time-Dependent Partition-Free Approach in Resonant Tunneling Systems. *Phys. Rev. B: Condens. Matter Mater. Phys.* **2004**, *69*, 195318.
- (34) Kurth, S.; Stefanucci, G.; Almbladh, C. O.; Rubio, A.; Gross, E. K. U. Time-Dependent Quantum Transport: A Practical Scheme Using Density Functional Theory. *Phys. Rev. B: Condens. Matter Mater. Phys.* **2005**, *72*, 035308.
- (35) Maciejko, J.; Wang, J.; Guo, H. Time-Dependent Quantum Transport Far From Equilibrium: An Exact Nonlinear Response Theory. *Phys. Rev. B: Condens. Matter Mater. Phys.* **2006**, *74*, 085324.
- (36) Galperin, M.; Tretiak, S. Linear Optical Response of Current-Carrying Molecular Junction: A Nonequilibrium Green's Function-Time-Dependent Density Functional Theory Approach. *J. Chem. Phys.* **2008**, *128*, 124705.
- (37) Zheng, X.; Chen, G.; Mo, Y.; Koo, S.; Tian, H.; Yam, C.; Yan, Y. Time-Dependent Density Functional Theory for Quantum Transport. *J. Chem. Phys.* **2010**, *133*, 114101.
- (38) Wang, R.; Hou, D.; Zheng, X. Time-Dependent Density-Functional Theory for Real-Time Electronic Dynamics on Material Surfaces. *Phys. Rev. B: Condens. Matter Mater. Phys.* **2013**, *88*, 205126.
- (39) Stefanucci, G.; Almbladh, C.-O. Time-Dependent Quantum Transport: An Exact Formulation Based on TDDFT. *Europhys. Lett.* **2004**, *67*, 14–20.
- (40) Mühlbacher, L.; Rabani, E. Real-Time Path Integral Approach to Nonequilibrium Many-Body Quantum Systems. *Phys. Rev. Lett.* **2008**, *100*, 176403.
- (41) Cohen, G.; Rabani, E. Memory Effects in Nonequilibrium Quantum Impurity Models. *Phys. Rev. B: Condens. Matter Mater. Phys.* **2011**, *84*, 075150.
- (42) Cohen, G.; Gull, E.; Reichman, D. R.; Millis, A. J.; Rabani, E. Numerically Exact Long-Time Magnetization Dynamics at the Nonequilibrium Kondo Crossover of the Anderson Impurity Model. *Phys. Rev. B: Condens. Matter Mater. Phys.* **2013**, *87*, 195108.
- (43) Wang, H.; Thoss, M. Numerically Exact, Time-Dependent Study of Correlated Electron Transport in Model Molecular Junctions. *J. Chem. Phys.* **2013**, *138*, 134704.
- (44) Wang, H.; Thoss, M. Multilayer Multiconfiguration Time-Dependent Hartree Study of Vibrationally Coupled Electron Transport Using the Scattering-State Representation. *J. Phys. Chem. A* **2013**, *117*, 7431–7441.
- (45) Baer, R.; Neuhauser, D. Ab Initio Electrical Conductance of a Molecular Wire. *Int. J. Quantum Chem.* **2003**, *91*, 524–532.
- (46) Baer, R.; Seideman, T.; Ilani, S.; Neuhauser, D. Ab Initio Study of the Alternating Current Impedance of a Molecular Junction. *J. Chem. Phys.* **2004**, *120*, 3387–3396.
- (47) Varga, K. Time-Dependent Density Functional Study of Transport in Molecular Junctions. *Phys. Rev. B: Condens. Matter Mater. Phys.* **2011**, *83*, 195130.
- (48) Zhou, Z.; Chu, S.-I. A Time-Dependent Momentum-Space Density Functional Theoretical Approach for Electron Transport Dynamics in Molecular Devices. *Europhys. Lett.* **2009**, *88*, 17008.
- (49) Di Ventura, M.; D'Agosta, R. Stochastic Time-Dependent Current-Density-Functional Theory. *Phys. Rev. Lett.* **2007**, *98*, 226403.
- (50) D'Agosta, R.; Di Ventura, M. Stochastic Time-Dependent Current-Density-Functional Theory: A Functional Theory of Open Quantum Systems. *Phys. Rev. B: Condens. Matter Mater. Phys.* **2008**, *78*, 165105.
- (51) Appel, H.; Di Ventura, M. Stochastic Quantum Molecular Dynamics. *Phys. Rev. B: Condens. Matter Mater. Phys.* **2009**, *80*, 212303.
- (52) Appel, H.; Ventura, M. D. Stochastic Quantum Molecular Dynamics for Finite and Extended Systems. *Chem. Phys.* **2011**, *391*, 27–36.
- (53) Biele, R.; D'Agosta, R. A Stochastic Approach to Open Quantum Systems. *J. Phys.: Condens. Matter* **2012**, *24*, 273201.
- (54) Hofmann-Mees, D.; Appel, H.; Di Ventura, M.; Kummel, S. Determining Excitation-Energy Transfer Times and Mechanisms from Stochastic Time-Dependent Density Functional Theory. *J. Phys. Chem. B* **2013**, *117*, 14408–14419.
- (55) Katz, G.; Gelman, D.; Ratner, M. A.; Kosloff, R. Stochastic Surrogate Hamiltonian. *J. Chem. Phys.* **2008**, *129*, 034108.
- (56) Burke, K.; Car, R.; Gebauer, R. Density Functional Theory of the Electrical Conductivity of Molecular Devices. *Phys. Rev. Lett.* **2005**, *94*, 146803.
- (57) Gebauer, R.; Car, R. Electron Transport with Dissipation: A Quantum Kinetic Approach. *Int. J. Quantum Chem.* **2005**, *101*, 564–571.
- (58) Bodor, A.; Diósi, L. Conserved Current in Markovian Open-Quantum Systems. *Phys. Rev. A: At, Mol, Opt. Phys.* **2006**, *73*, 064101.
- (59) Gebauer, R.; Burke, K.; Car, R. Kohn-Sham Master Equation Approach to Transport Through Single Molecules Time-Dependent Density Functional Theory. In *Lecture Notes in Physics*; Marques, M., Ullrich, C., Nogueira, F., Rubio, A., Burke, K., Gross, E., Eds.; Springer: Berlin, 2006; Vol. 706, pp 463–477.
- (60) Koentopp, M.; Chang, C.; Burke, K.; Car, R. Density Functional Calculations of Nanoscale Conductance. *J. Phys.: Condens. Matter* **2008**, *20*, 083203.
- (61) Gebauer, R.; Piccinin, S.; Car, R. Quantum Collision Current in Electronic Circuits. *ChemPhysChem* **2005**, *6*, 1727–1730.
- (62) Frenslley, W. R. Boundary Conditions for Open Quantum Systems Driven Far From Equilibrium. *Rev. Mod. Phys.* **1990**, *62*, 745–791.
- (63) Gebauer, R.; Car, R. Current in Open Quantum Systems. *Phys. Rev. Lett.* **2004**, *93*, 160404.
- (64) Li, X.-Q.; Yan, Y. Quantum Master Equation Scheme of Time-Dependent Density Functional Theory to Time-Dependent Transport in Nanoelectronic Devices. *Phys. Rev. B: Condens. Matter Mater. Phys.* **2007**, *75*, 075114.
- (65) Zheng, X.; Wang, F.; Yam, C. Y.; Mo, Y.; Chen, G. Time-Dependent Density-Functional Theory for Open Systems. *Phys. Rev. B: Condens. Matter Mater. Phys.* **2007**, *75*, 195127.
- (66) Wang, Y.; Yam, C. Y.; Frauenheim, T.; Chen, G. H.; Niehaus, T. A. An Efficient Method for Quantum Transport Simulations in the Time Domain. *Chem. Phys.* **2011**, *391*, 69–77.
- (67) Koo, S. K.; Yam, C. Y.; Zheng, X.; Chen, G. First-Principles Liouville–von Neumann Equation for Open Systems and its Applications. *Phys. Status Solidi B* **2012**, *249*, 270–275.
- (68) Di Ventura, M.; Todorov, T. N. Transport in Nanoscale Systems: the Microcanonical versus Grand-Canonical Picture. *J. Phys.: Condens. Matter* **2004**, *16*, 8025–8034.
- (69) Ajisaka, S.; Barra, F.; Zunkovic, B. Nonequilibrium Quantum Phase Transitions in the XY Model: Comparison of Unitary Time

Evolution and Reduced Density Operator Approaches. *New J. Phys.* **2014**, *16*, 033028.

(70) Ajisaka, S.; Barra, F.; Mejía-Monasterio, C.; Prosen, T. Nonequilibrium Particle and Energy Currents in Quantum Chains Connected to Mesoscopic Fermi Reservoirs. *Phys. Rev. B: Condens. Matter Mater. Phys.* **2012**, *86*, 125111.

(71) Ajisaka, S.; Barra, F. Nonequilibrium Mesoscopic Fermi-Reservoir Distribution and Particle Current Through a Coherent Quantum System. *Phys. Rev. B: Condens. Matter Mater. Phys.* **2013**, *87*, 195114.

(72) Caspary Toroker, M.; Peskin, U. A Quantum Mechanical Flux Correlation Approach to Steady-State Transport Rates in Molecular Junctions. *Chem. Phys.* **2010**, *370*, 124–131.

(73) Bushong, N.; Gamble, J.; Di Ventra, M. Electron Turbulence at Nanoscale Junctions. *Nano Lett.* **2007**, *7*, 1789–1792.

(74) Bushong, N.; Sai, N.; Di Ventra, M. Approach to Steady-State Transport in Nanoscale Conductors. *Nano Lett.* **2005**, *5*, 2569–2572.

(75) Cheng, C.-L.; Evans, J. S.; Van Voorhis, T. Simulating Molecular Conductance Using Real-Time Density Functional Theory. *Phys. Rev. B: Condens. Matter Mater. Phys.* **2006**, *74*, 155112.

(76) Evans, J. S.; Cheng, C.-L.; Van Voorhis, T. Spin-Charge Separation in Molecular Wire Conductance Simulations. *Phys. Rev. B: Condens. Matter Mater. Phys.* **2008**, *78*, 165108.

(77) Evans, J. S.; Voorhis, T. V. Dynamic Current Suppression and Gate Voltage Response in Metal–Molecule–Metal Junctions. *Nano Lett.* **2009**, *9*, 2671–2675.

(78) Ercan, I.; Anderson, N. G. Tight-Binding Implementation of the Microcanonical Approach to Transport in Nanoscale Conductors: Generalization and Analysis. *J. Appl. Phys.* **2010**, *107*, 124318.

(79) Sánchez, C. G.; Stamenova, M.; Sanvito, S.; Bowler, D. R.; Horsfield, A. P.; Todorov, T. N. Molecular Conduction: Do Time-Dependent Simulations Tell You More Than the Landauer Approach? *J. Chem. Phys.* **2006**, *124*, 214708.

(80) Rothman, A. E.; Mazziotti, D. A. Nonequilibrium, Steady-State Electron Transport with N-Representable Density Matrices from the Anti-Hermitian Contracted Schrödinger Equation. *J. Chem. Phys.* **2010**, *132*, 104112.

(81) Subotnik, J. E.; Hansen, T.; Ratner, M. A.; Nitzan, A. Nonequilibrium Steady State Transport via the Reduced Density Matrix Operator. *J. Chem. Phys.* **2009**, *130*, 144105–144116.

(82) Jin, J.; Zheng, X.; Yan, Y. Exact Dynamics of Dissipative Electronic Systems and Quantum Transport: Hierarchical Equations of Motion Approach. *J. Chem. Phys.* **2008**, *128*, 234703.

(83) Sakurai, A.; Tanimura, Y. An Approach to Quantum Transport Based on Reduced Hierarchy Equations of Motion: Application to a Resonant Tunneling Diode. *J. Phys. Soc. Jpn.* **2013**, *82*, 033707.

(84) Xie, H.; Jiang, F.; Tian, H.; Zheng, X.; Kwok, Y.; Chen, S.; Yam, C.; Yan, Y.; Chen, G. Time-Dependent Quantum Transport: An Efficient Method Based on Liouville-von-Neumann Equation for Single-Electron Density Matrix. *J. Chem. Phys.* **2012**, *137*, 044113.

(85) Timm, C. Tunneling Through Molecules and Quantum Dots: Master-Equation Approaches. *Phys. Rev. B: Condens. Matter Mater. Phys.* **2008**, *77*, 195416.

(86) Croy, A.; Saalman, U. Propagation Scheme for Nonequilibrium Dynamics of Electron Transport in Nanoscale Devices. *Phys. Rev. B: Condens. Matter Mater. Phys.* **2009**, *80*, 245311.

(87) Popescu, B.; Kleinekathöfer, U. Treatment of Time-Dependent Effects in Molecular Junctions. *Phys. Status Solidi B* **2013**, *250*, 2288–2297.

(88) Zhang, W.-M.; Lo, P.-Y.; Xiong, H.-N.; Tu, M. W.-Y.; Nori, F. General Non-Markovian Dynamics of Open Quantum Systems. *Phys. Rev. Lett.* **2012**, *109*, 170402.

(89) Suess, D.; Strunz, W. T.; Eisfeld, A. Hierarchical Equations for Open System Dynamics in Fermionic and Bosonic Environments. *J. Stat. Phys.* **2015**, *159*, 1408–1423.

(90) Nguyen, T. S.; Nanguneri, R.; Parkhill, J. How Electronic Dynamics with Pauli Exclusion Produces Fermi–Dirac Statistics. *J. Chem. Phys.* **2015**, *142*, 134113.

(91) Zelovich, T.; Kronik, L.; Hod, O. State Representation Approach for Atomistic Time-Dependent Transport Calculations in Molecular Junctions. *J. Chem. Theory Comput.* **2014**, *10*, 2927–2941.

(92) Zelovich, T.; Kronik, L.; Hod, O. Molecule–Lead Coupling at Molecular Junctions: Relation between the Real- and State-Space Perspectives. *J. Chem. Theory Comput.* **2015**, *11*, 4861–4869.

(93) Chen, L. P.; Hansen, T.; Franco, I. Simple and Accurate Method for Time-Dependent Transport along Nanoscale Junctions. *J. Phys. Chem. C* **2014**, *118*, 20009–20017.

(94) Kossakowski, A. On Quantum Statistical Mechanics of Non-Hamiltonian Systems. *Rep. Math. Phys.* **1972**, *3*, 247–274.

(95) Gorini, V.; Kossakowski, A.; Sudarshan, E. C. G. Completely Positive Dynamical Semigroups of N-level systems. *J. Math. Phys.* **1976**, *17*, 821–825.

(96) Lindblad, G. On the Generators of Quantum Dynamical Semigroups. *Commun. Math. Phys.* **1976**, *48*, 119–130.

(97) Head-Marsden, K.; Mazziotti, D. A. Communication: Satisfying Fermionic Statistics in the Modeling of Open Time-Dependent Quantum Systems with One-Electron Reduced Density Matrices. *J. Chem. Phys.* **2015**, *142*, 051102.

(98) Dubi, Y.; Di Ventra, M. Thermoelectric Effects in Nanoscale Junctions. *Nano Lett.* **2009**, *9*, 97–101.

(99) The initial conditions employed include equilibrium Fermi–Dirac distributions in the left and right leads with the corresponding chemical potentials (given by the lead Fermi energy plus or minus half the bias voltage) and temperatures and a similar single-particle state occupation distribution in the extended molecule manifold with its chemical potential set to the Fermi energy of the whole finite model system at equilibrium and a preset initial temperature.